ORIGINAL ARTICLE

On the rotational dynamics of Prometheus and Pandora

A. V. Melnikov · I. I. Shevchenko

Abstract   Possible rotation states of two satellites of Saturn, Prometheus (S16) and Pandora (S17), are studied by means of numerical experiments. The attitude stability of all possible modes of synchronous rotation and the motion close to these modes is analyzed by means of computation of the Lyapunov spectra of the motion. The stability analysis confirms that the rotation of Prometheus and Pandora might be chaotic, though the possibility of regular behaviour is not excluded. For the both satellites, the attitude instability zones form series of concentric belts enclosing the main synchronous resonance center in the phase space sections. A hypothesis is put forward that these belts might form "barriers" for capturing the satellites in synchronous rotation. The satellites in chaotic rotation can mimic ordinary regular synchronous behaviour: they preserve preferred orientation for long periods of time, the largest axis of satellite's figure being directed approximately towards Saturn.

Keywords   Resonances · Chaotic motion · Rotational dynamics · Satellites of Saturn: Prometheus, Pandora · Chaotic satellite rotation

1 Introduction

In 1980s, Wisdom et al. (1984) and Wisdom (1987) demonstrated theoretically that a planetary satellite of non-spherical shape in an elliptic orbit can rotate in a chaotic, unpredictable way. They found that the most probable candidate for the chaotic rotation, due to pronounced shape asymmetry and significant orbital eccentricity, was the satellite of Saturn Hyperion (S7). Later on, a direct modelling of observed light curves of Hyperion (Klavetter 1989a,b, Thomas et al. 1995, Black et al. 1995, Devyatkin et al. 2002) confirmed the chaotic character of its rotation.

A. V. Melnikov (✉) · I. I. Shevchenko
Pulkovo Observatory of the Russian Academy of Sciences, Pulkovskoje ave. 65-1,
196140 St. Petersburg, Russia
e-mail: melnikov@gao.spb.ru

Recently it was found in a theoretical research (Kouprianov and Shevchenko 2005), that two other satellites of Saturn, Prometheus (S16) and Pandora (S17), can also reside in a state of chaotic rotation. Contrary to the case of Hyperion, chaos in rotation of these two satellites is due to fine-tuning of the dynamical and physical parameters rather than simply to a large extent of a chaotic zone in the rotational phase space.

It is remarkable that the orbital dynamics of Prometheus and Pandora are known to be chaotic with the Lyapunov time of only 3 years, and this dynamical chaos is directly observed (see Goldreich and Rappaport 2003a,b, Cooper and Murray 2004, Farmer and Goldreich 2006). However note that the theoretical inferences on chaos in rotation of these satellites are completely independent from the existence of orbital chaos.

In the present paper we study the problem of rotational dynamics of these two satellites in detail, exploring the attitude stability not only in the centers of synchronous resonances, but also in the phase space in the vicinities of the resonances. Our analysis includes period-doubling bifurcation modes of synchronous spin–orbit states. We take into account all available modern observational data.

An important problem, first of all from the observational point of view, is the following: whether there exists a preferred orientation of the satellites rotating chaotically, or all orientations are equiprobable? The orientation of a satellite in chaotic rotation, generally speaking, is not necessarily isotropic. This was demonstrated in a numerical experiment by Wisdom (1987) in calculating the rotation of Phobos in the vicinities of the separatrices of the 1:2 spin–orbit resonance (see Fig. 5 in Wisdom 1987).

The plan of the present work is as follows. First, we study the attitude stability of the planar rotation of Prometheus and Pandora with respect to tilting the axis of rotation. The stability analysis is carried out for all possible exact modes of synchronous resonance (α-resonance, β-resonance, and the period-doubling bifurcation mode of α-resonance), as well as for the trajectories of all possible kinds (periodic, quasiperiodic, chaotic in the planar problem) on a representative section of the phase space of planar rotation. Then the problem on the preferred orientation of Prometheus and Pandora in chaotic rotation is considered.

2 The reference frame and the equations of motion

We suppose that a satellite represents a non-spherical rigid body moving around a planet (a gravitating point) in a non-perturbed elliptic orbit with the eccentricity e. Location of the satellite in the orbit is determined by the true anomaly f or the eccentric anomaly E. The shape of the satellite is described by a triaxial ellipsoid with the principal semiaxes $a > b > c$ and the corresponding principal central moments of inertia $A < B < C$. The size of the satellite is much less than the radius of the orbital motion. The dynamics of the three-dimensional rotation of the satellite is determined by the parameters e, b/a, c/b and the initial conditions of the motion. The angular velocities of rotation are expressed in the units of the orbital mean motion, and the "satellite–planet" distance is expressed in the units of the semimajor axis of the orbit. One orbital period corresponds to 2π time units.

The oblateness of Saturn causes precession of the pericenters of the orbits of the satellites, the precession rate being equal to $3.1911 \times 10^{-5\circ}\mathrm{s}^{-1}$ in the case of Prometheus and $3.0082 \times 10^{-5\circ}\mathrm{s}^{-1}$ in the case of Pandora (Goldreich and Rappaport 2003b). Hence the periods of precession are equal to 0.36 and 0.38 year, respectively. This is much greater that the Lyapunov times (<1 d; see Kouprianov and Shevchenko 2005) of the rotation of these satellites, if it were chaotic. Since the timescales are so different, we ignore the precession of orbits in our study.

For describing the orientation of the satellite we use an inertial frame identical to that used in Wisdom et al. (1984) and Melnikov and Shevchenko (1998, 2000). This $Oxyz$ frame is defined initially at the pericenter of the orbit as follows: the x axis is directed along the "orbit pericenter–planet" vector, the y axis is parallel to the vector of the orbital velocity at the pericenter, the z axis is orthogonal to the orbital plane and completes the reference system to a right-handed system. Orientation of the satellite with respect to the axes of the $Oxyz$ frame is defined by a sequence of imaginary rotations of the satellite by the Euler angles θ, ϕ, ψ from an initial position until the satellite reaches its actual orientation. In the initial position the axes a, b, c coincide with the axes x, y, z, respectively. The axes a, b, c are directed along the principal axes of inertia with the moments A, B, C, respectively, and are "frozen" in the satellite. The imaginary rotations are carried out in the following sequence: first, rotation by θ about c, second, rotation by ϕ about a, and third, rotation by ψ about b.

The definition of the Euler angles adopted here is identical to that described and used by Wisdom et al. (1984) and is different from the usual one. The reason for using the alternative Euler angle set is that the standard one has a coordinate singularity at the point where a satellite's c axis (the axis of the maximum moment of inertia) is orthogonal to the orbit plane. In the adopted frame this position corresponds to $\phi = 0$, while the singularity is shifted to $\phi = \pm\pi/2$. The latter value corresponds to the satellite's axis of rotation lying in the orbit plane.

Rotation of the satellite is described by Euler's dynamic and kinematic equations. The dynamic equations (Beletsky 1965, Wisdom et al. 1984) can be written as

$$\begin{cases} A\frac{d\omega_a}{dt} - \omega_b\omega_c(B-C) = -3\frac{GM}{r^3}\beta\gamma(B-C), \\ B\frac{d\omega_b}{dt} - \omega_c\omega_a(C-A) = -3\frac{GM}{r^3}\gamma\alpha(C-A), \\ C\frac{d\omega_c}{dt} - \omega_a\omega_b(A-B) = -3\frac{GM}{r^3}\alpha\beta(A-B). \end{cases} \quad (1)$$

Here G is the gravitational constant; M is the mass of the planet; ω_a, ω_b, ω_c are the projections of the vector of the angular velocity $\boldsymbol{\omega}$ on the axes a, b, c; $r = a(1 - e\cos E)$ is the "satellite—planet" distance, a is the semimajor axis of the orbit; α, β, γ are the direction cosines of the principal axes of inertia with respect to the direction to the planet.

The kinematic equations and expressions for direction cosines, in the reference frame used here, according to (Wisdom et al. 1984, Melnikov and Shevchenko 1998), are given by

$$\begin{cases} \omega_a = \frac{d\theta}{dt}\sin\phi\sin\psi + \frac{d\phi}{dt}\cos\psi, \\ \omega_b = \frac{d\theta}{dt}\sin\phi\cos\psi - \frac{d\phi}{dt}\sin\psi, \\ \omega_c = \frac{d\theta}{dt}\cos\phi + \frac{d\psi}{dt}, \end{cases} \quad (2)$$

$$\begin{cases} \alpha = \cos(\theta - f)\cos\psi - \sin(\theta - f)\cos\phi\sin\psi, \\ \beta = -\cos(\theta - f)\sin\psi - \sin(\theta - f)\cos\phi\cos\psi, \\ \gamma = \sin(\theta - f)\cos\phi. \end{cases} \quad (3)$$

Eqs. 1–3 are used in what follows for calculation of the rotational dynamics.

3 Synchronous resonance regimes and attitude stability of rotation

3.1 The "Amalthea effect"

In Melnikov and Shevchenko (1998, 2000) it was found for Amalthea (J5) that two different synchronous regimes of rotation, "α-resonance" and "β-resonance", coexist in the phase

space of rotation of this satellite. By means of calculation of the Lyapunov characteristic exponents (LCEs), Melnikov and Shevchenko (1998) showed that the planar rotation of Amalthea in the β-resonance center and its neighbourhood was stable with respect to tilting the axis of rotation, while its rotation in the α-resonance center and its neighbourhood was unstable. (Note that the terms "α-resonance" and "β-resonance" had not yet been used in that paper.) In Melnikov and Shevchenko (2000) by means of calculation and statistical analysis of the multipliers of the periodic solutions corresponding to the α- and β-resonances, the stability of rotation of Amalthea at the centers of the both modes was investigated on a grid of values of the inertial parameters. The conclusion was made that Amalthea could not reside in α-resonance.

Let us introduce the parameter $\omega_0 = \sqrt{3(B - A)/C}$, which is the frequency of small-amplitude oscillations of a satellite in synchronous resonance (see Wisdom et al. 1984, Shevchenko 1999). It roughly characterizes the dynamical asymmetry of the satellite shape. If we accept the data of EA (1999), then $\omega_0 = 1.058$ for Prometheus and $\omega_0 = 0.812$ for Pandora.

For two centers of synchronous resonance to coexist in the phase space of rotational motion (the "Amalthea effect"), the ω_0 parameter must exceed unity slightly; see Figs. 1 and 2 in Melnikov and Shevchenko (2000) and also Fig. 3 in the present paper. Note that, in addition, the orbital eccentricity must obey a certain constraint: it must not be too high. The limit on the eccentricity, which allows coexistence of the periodic solutions corresponding to

Fig. 1 **(a)** Location of the satellites with known values of the shape parameters in the "$e-\omega_0$" diagram. **(b)** Location of Prometheus (crosses) and Pandora (circles) in the diagram "$e-\omega_0$" according to Table 1
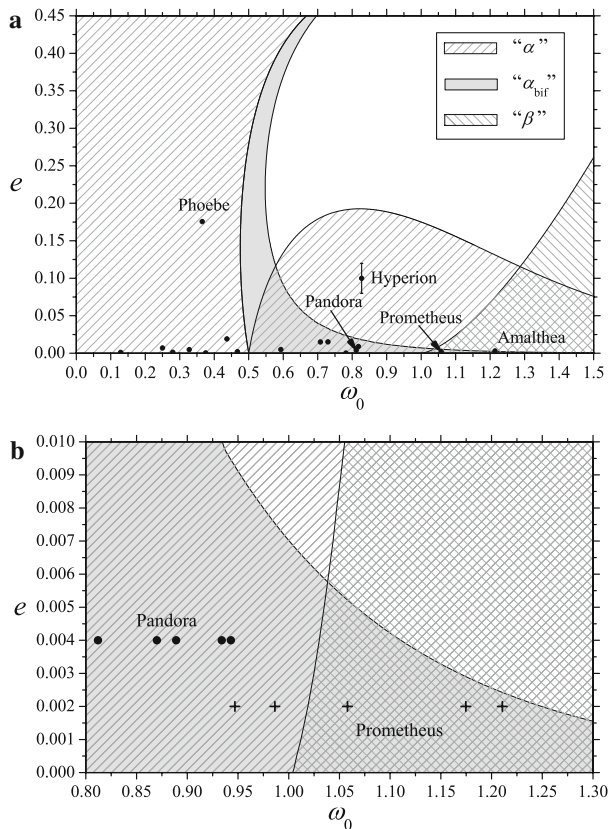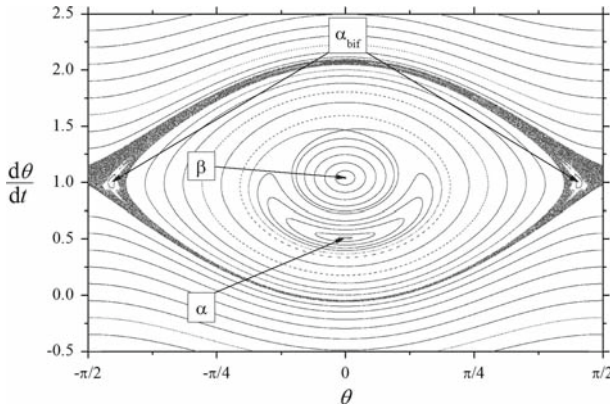
Fig. 2 The phase space section of the planar rotational motion of Prometheus. The exact synchronous resonance modes are indicated
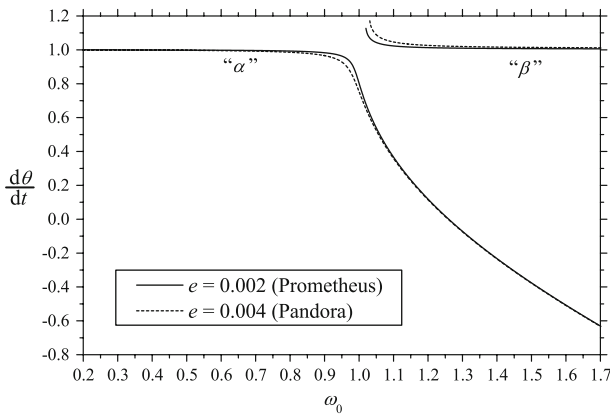

Fig. 3 The $d\theta/dt$ coordinates of the centers of synchronous resonance in the phase space section in dependence on the ω_0 parameter. The curves starting on the left side of the plot correspond to α-resonance, those starting on the right side correspond to β-resonance

α-resonance and β-resonance, is as follows: $e < \frac{4\sqrt{3}}{9}(\omega_0 - 1)^{3/2}$ (Beletsky 1965, Chap. 2; Markeev 1990, p. 366).

The "Amalthea effect" takes place for prolate satellites. Indeed, $\omega_0 = \sqrt{3(B - A)/C} = \sqrt{3(a^2 - b^2)/(a^2 + b^2)}$ for a triaxial ellipsoid with homogeneous density (see Kouprianov and Shevchenko 2006, p. 396). The parameter $\omega_0 > 1$ if $c < b < a/\sqrt{2}$. In other words, two semiaxes should be less than ≈ 0.7 of the third one. The "Amalthea effect" was considered and discussed in detail in Kouprianov and Shevchenko (2006) and Melnikov and Shevchenko (2007). It was shown that this effect might be abundant amongst minor planetary satellites (the satellites with diameters < 100 km) moving in close-to-circular orbits.

3.2 Synchronous states: α-resonance, β-resonance and period-doubling bifurcation mode of α-resonance

The available data on the parameters of the figures of Prometheus and Pandora are collected in Table 1. Note that the data on the shapes of Prometheus and Pandora derived by Thomas

Table 1 The shape parameters for Prometheus and Pandora

Prometheus (S16)		Pandora (S17)		References
b/a	c/b	b/a	c/b	
0.714	0.740	0.764	0.786	Wisdom (1987)
0.676	0.680	0.800	0.705	Thomas (1989)
0.586	0.706	0.737	0.738	Stooke (1993)
0.608	0.726	0.741	0.782	Goździewski and Maciejewski (1995)
0.676	0.680	0.800	0.705	EA (1999)
0.734	0.696	0.773	0.804	Porco et al. (2006)

(1989) are tabulated in the reports by Seidelmann et al. (2002, 2005, 2007). Besides, the data on the adopted positions of the poles of Prometheus and Pandora can be found in these reports; these data are the same in the three references. We set the orbital eccentricity equal to $e = 0.002$ for Prometheus and $e = 0.004$ for Pandora, as in EA (1999). According to (Goldreich and Rappaport, 2003a, Figs. 5 and 6), on the timescale of 20 years the eccentricity of Prometheus varies in the limits 2.27×10^{-3}–2.30×10^{-3}, and that of Pandora in the limits 4.35×10^{-3}–4.38×10^{-3} (see also French et al. 2003).

The "e–ω_0" diagram for the satellites with known values of the shape parameters, based on the data compiled in Kouprianov and Shevchenko (2005), is shown in Fig. 1a. The theoretical boundaries of the zones of existence of α-resonance, β-resonance, and period-doubling bifurcation mode α_{bif} of α-resonance are indicated according to the data in Melnikov (2001).

As follows from Fig. 1a, period-doubling bifurcation mode α_{bif} of α-resonance can be present in the phase space of rotation of Prometheus and Pandora. For Pandora, this confirms an earlier analysis by Melnikov (2001) made on the basis of a single estimate of the inertial parameters. In Fig. 1b, a part of the "e–ω_0" diagram with location of Prometheus and Pandora indicated according to the data of Table 1 is given in higher resolution. In the case of Pandora, β-resonance does not exist for all the data considered. In the case of Prometheus, β-resonance does not exist only for the data due to Wisdom (1987) and Porco et al. (2006). According to all other sources, Prometheus lies in the zone of existence of this mode. For all the data on Prometheus and Pandora, period-doubling bifurcation mode of α-resonance exists.

In Fig. 2, the phase space section of the planar rotational motion of Prometheus is shown. The section is defined at the pericenter of the orbit; i.e., the variables are mapped each orbital period. Note that the planar problem (that with $\phi = \psi = 0$) has one and a half degrees of freedom. The center of α-resonance (the lower one in the section) and that of β-resonance (the upper one) are indicated in the section. Besides, there is period-doubling bifurcation mode α_{bif}, that manifests itself in the two prominent regular islands inside the chaotic layer at the left and at the right sides from the center of β-resonance.

We see that Prometheus is subject to the "Amalthea effect". In a different terminology this was noted in Melnikov (2001). What is more, period-doubling bifurcation mode of α-resonance is possible for this satellite, i.e., the potentially possible rotational dynamics are very rich.

3.3 Attitude stability of exact synchronous rotation

Let us consider the stability of synchronous rotation of Prometheus and Pandora with respect to tilting the axis of rotation in the cases of exact α-resonance, β-resonance, and

period-doubling bifurcation mode α_{bif}. Melnikov and Shevchenko (2000) and Kouprianov and Shevchenko (2005) performed a research of the stability on the $(A/C, B/C)$ plane. Here we use another plane, namely, the $(c/b, b/a)$ plane[1], which is more graphical.

In the cases of α-resonance and β-resonance we use a method based on the analysis of the modal structure of the differential distribution of the computed modules of multipliers of periodic solutions of the equations of motion. The method is described in detail in Melnikov and Shevchenko (2000).

In the considered problem, the system of equations of motion in variations with respect to the periodic solution consists of six linear differential equations of the first order with periodic coefficients. Numerical integration of the system allows one to obtain the matrix of linear transformation of variations for one period (see Wisdom et al. 1984). The periodic solutions in the given problem are characterized by three pairs of multipliers. The distributions of the modules of multipliers are built for a set of trajectories corresponding to a center of synchronous resonance on a grid of values of the b/a and c/b parameters. Analysis of the distributions (see Melnikov and Shevchenko 2000) allows one to separate orbits stable with respect to tilting the axis of rotation from those which are unstable.

Analysis of the attitude stability of period-doubling bifurcation mode α_{bif} is carried out by means of computation of the whole spectrum of the LCEs for a set of values of the b/a and c/b parameters, followed by analysis of the differential distributions of the computed values of the LCEs. By means of a similar method we investigated the stability of rotation of planetary satellites (Melnikov and Shevchenko 1998) on sets of initial data of the trajectories. Here the distributions of the LCE values for the trajectories with the initial data taken at exact period-doubling bifurcation mode α_{bif} are built on a grid of values of the b/a and c/b parameters. We set the grid resolution equal to 0.001 in both b/a and c/b axes. Analysis of the modal structure of the distributions allows one to separate the stable trajectories, for which all three indices are zero, and the unstable ones for which at least one of the LCEs is distinct from zero.

The true values of the LCEs are supposed to be the limits of the computed values when the time of computation tends to infinity. The time of computation is necessarily finite. However, it is implied henceforth that the obtained numerical values in the case of chaotic trajectories represent the true LCE values, because the time of computation was taken to be long enough for the computed LCEs of the chaotic trajectories to saturate (i.e., increasing the computation time would not make the computed LCE values less; a "plateau" is reached in each case). In what concerns the regular trajectories, the obtained numerical values of the LCEs tend to zero with increasing the computation time.

For the computation of the LCE spectra, we use the HQRB method (von Bremen et al. 1997), programmed as a software package in Shevchenko and Kouprianov (2002) and Kouprianov and Shevchenko (2003). The Dormand–Prince integrator DOPRI8 (Hairer et al. 1987), realizing in Fortran the 8th order Runge–Kutta method with the step size control, is used for integration of equations of motion (1), (2).

In Fig. 3, the $d\theta/dt$ coordinates of the centers of synchronous resonance in the phase space section in dependence on the ω_0 parameter are shown for the values of the orbital eccentricities of both satellites. The curves starting on the left side of the plot correspond to α-resonance, those starting on the right side correspond to β-resonance. As it is clear from Fig. 3, α- and β-resonances coexist in a substantial interval of ω_0, if the orbital eccentricities are so small. β-resonance is born at $\omega_0 \approx 1$; α-resonance disappears at a large value of ω_0, out

---

[1] We are grateful to A. Doborovolskis for the advice to use the given coordinates.

of the presented plot limit. The problem of bifurcations causing the birth and disappearance of α- and β-resonances is considered in brief by Melnikov and Shevchenko (2000).

The computed regions of stability and instability are shown in Fig. 4 (for Prometheus) and in Fig. 5 (for Pandora). The regions of stability are shown in light gray, the regions of minimum (one degree of freedom) instability are shown in dark gray, and the regions of maximum (two degrees of freedom) instability are shown in black. The lines of constant value of the ω_0 parameter are depicted for orientation.

It follows from the diagrams in Fig. 4a, b that α-resonance is attitude unstable for most of the observational data for Prometheus. Earlier this instability was noted in Melnikov (2001) and Kouprianov and Shevchenko (2005) on the basis of a single estimate of the inertial parameters. In the case of the data due to Porco et al. (2006), α-resonance is close to instability. Rotation of Prometheus in β-resonance is close to instability, in agreement with an inference by Kouprianov and Shevchenko (2005). In the case of Pandora (see Fig. 5a), rotation in α-resonance is close to instability for the data of Wisdom (1987), Thomas (1989) and Porco et al. (2006) and is unstable for the data of Stooke (1993) and Goździewski and Maciejewski (1995), in general agreement with Kouprianov and Shevchenko (2005), where the stability analysis was based on a single estimate of the inertial parameters.

From the diagrams in Figs. 4c and Fig. 5b it is clear that synchronous rotation in the α_{bif} mode is attitude unstable for both Prometheus and Pandora.

3.4 Attitude stability in the general case

Not only the stability in exact synchronous rotation is of interest. Let us study the attitude stability of the trajectories in the vicinities of the exact synchronous states on representative sets of initial data. Computation of the LCEs on a grid of initial data, followed by analysis of the distributions of the computed LCEc, enables one to accomplish such a study. A similar study with the use of the maximum LCEs was carried out in Melnikov and Shevchenko (1998) for Phobos, Deimos, Amalthea, and Hyperion. Here we study Prometheus and Pandora by means of analysis of the LCE spectra. Besides, we significantly increase the resolution of the initial data grid, as well as the time interval on which the LCEs are computed. For the surface of section we choose the $(\theta, d\theta/dt)$ plane taken at $t = 2\pi m$, $m = 0, 1, 2, \ldots$, i.e., defined at the orbit pericenter. In the computations we adopt the values of b/a and c/b as given in EA (1999) (see Table 1).

The computation of the LCEs has been carried out for two sets of trajectories, (i) and (ii), defined by the following choice of initial data: (i) $\theta = 0$, (ii) $\theta = \pi/2$; and in the both sets $d\theta/dt$ is taken in the range from -0.5 to 2.5 with the step equal to 0.003 in the case of Prometheus, and in the range from 0.0 to 2.0 with the step equal to 0.002 in the case of Pandora. The initial conditions also include $\phi = \psi = 0$, $d\phi/dt = d\psi/dt = 0$; the motion starts (i.e., $t = 0$) at the pericenter. Thus the LCEs have been computed for 2000 trajectories for each satellite.

Following Melnikov and Shevchenko (1998), in order to separate the regular and chaotic orbits, we build differential distributions of the computed LCE values. The distribution has two peaks; one of them corresponds to the chaotic orbits, and one to the regular orbits. On increasing the time interval of integration, the peak corresponding to the chaotic orbits remains motionless, while the abscissa of the peak corresponding to the regular orbits tends to zero (or to minus infinity in the logarithmic scale). Thus the sets of regular and chaotic trajectories are separated. The abscissa of a point between the peaks gives the numeric criterion for separation of the sets. Increasing the time interval of integration allows one to make this numeric criterion more precise.

Fig. 4 Regions of stability and instability with respect to tilting the axis of rotation; $e = 0.002$ (Prometheus): **(a)** for the center of α-resonance, **(b)** for the center of β-resonance, **(c)** for the exact period-doubling bifurcation mode of α-resonance. The locations of Prometheus according to the data of Table 1 are indicated by crosses
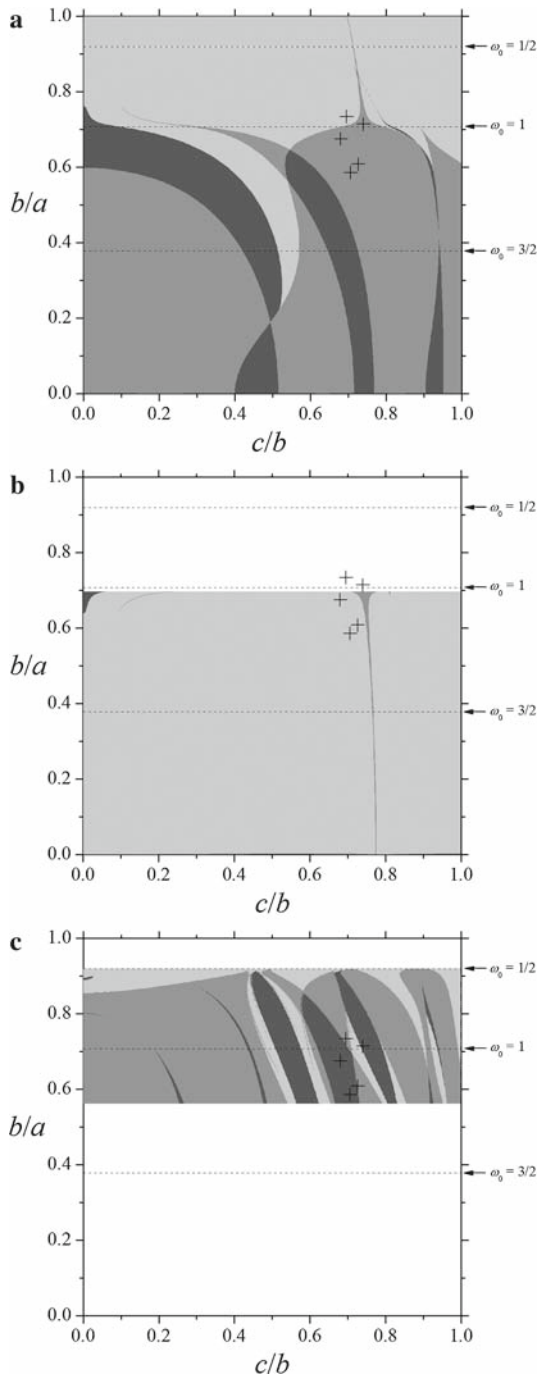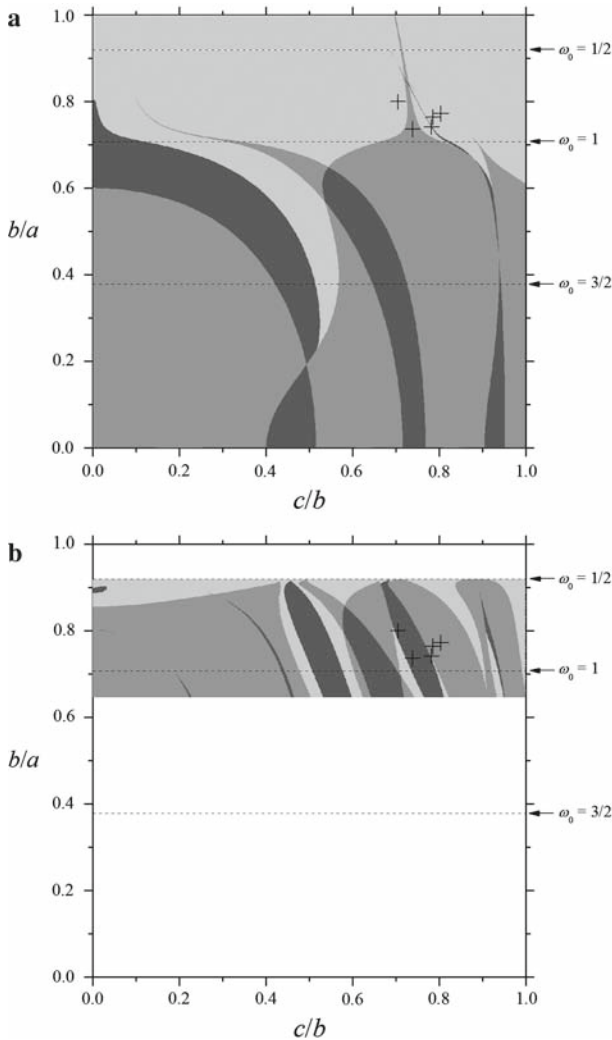
Fig. 5 Regions of stability and instability with respect to tilting the axis of rotation; $e = 0.004$ (Pandora): **(a)** for the center of α-resonance, **(b)** for the exact period-doubling bifurcation mode of α-resonance. The locations of Pandora according to the data of Table 1 are indicated by crosses

The LCE dependences on the initial value of $d\theta/dt$ in the case of $\theta = 0$ are shown in Fig. 6. They have been computed on the time intervals $t = 10^4$ and 10^5. From the plots it is clear that with increasing the integration time the computed LCE values for the chaotic trajectories remain constant, while the computed LCE values for the regular trajectories decrease. The horizontal dashed lines in the plots correspond to the adopted value of the LCE decimal logarithm (equal to -3 in all cases) separating the chaotic and regular trajectories. This criterion has been derived by means of building the distributions of the computed values of the LCEs at $t = 10^5$. It separates the peaks corresponding to the chaotic and regular trajectories in the distributions.

The separation of the regular and chaotic orbits, accomplished by means of analysis of the LCE distributions, allows one to build two variants of the phase space section, one for all

Fig. 6 The dependence of the LCEs on initial data. **(a)** $e = 0.002$, $\omega_0 = 1.058$ (Prometheus); **(b)** $e = 0.004$, $\omega_0 = 0.812$ (Pandora). The gray curves correspond to the computation time $t = 10^4$, the black curves to $t = 10^5$. The horizontal dashed lines correspond to the adopted value of the LCE decimal logarithm (equal to -3 in all cases) separating the chaotic and regular trajectories
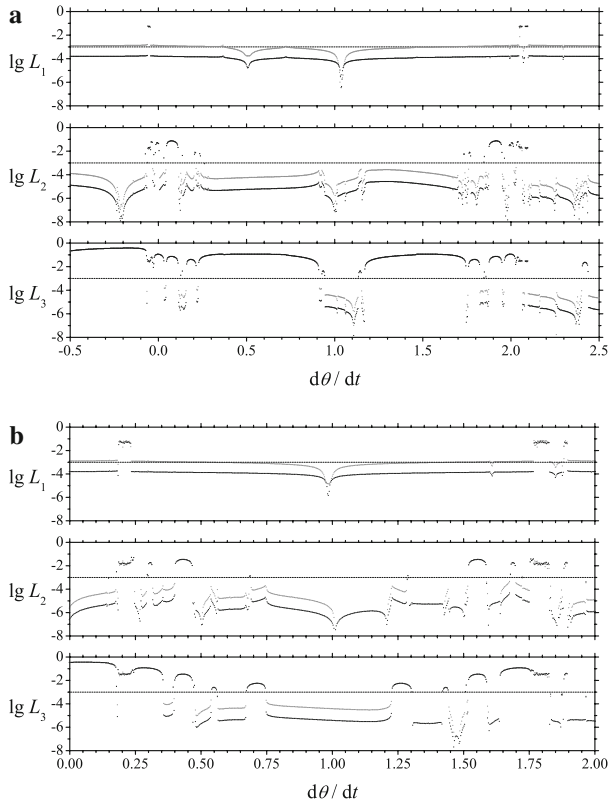
trajectories, and the other one only for the attitude stable trajectories. These double variants are shown for Prometheus in Figs. 7a, b, and for Pandora in Figs. 8a, b. The phase space sections for all trajectories are shown in Figs. 7a, 8a, while those for the attitude stable trajectories solely are shown in Figs. 7b and 8b. In order that structure of the section containing all trajectories were clearly discernible, it is constructed with a relatively low resolution of the initial data grid.

In the case of Prometheus (Figs. 2, 7a), there are two centers of synchronous resonance: α-resonance (the lower one in the section) and β-resonance (the upper one). Besides, there exists period-doubling bifurcation mode α_{bif}, located inside the chaotic layer at the left and right sides of the center of β-resonance. The librational trajectories are attitude stable only in the nearest neighbourhood of the center of β-resonance. Alternation of ring-like zones of stable and unstable motion is clearly seen for the librational trajectories enclosing the major synchronous state. This alternation is also clearly noticeable in Fig. 6a, where the computed values of the LCEs are given in function of the initial $d\theta/dt$ value. A broad band of quasiperiodic trajectories under the lower branch of the basic chaotic layer is attitude unstable. On the contrary, the motion above the upper branch of the layer is stable.

In the case of Pandora (Fig. 8), there exists period-doubling bifurcation mode α_{bif} located inside the chaotic layer at the left and right sides of the center of α-resonance. Alternation of ring-like zones of attitude stable and unstable librational trajectories enclosing the main synchronous state is even more pronounced than in the case of Prometheus.
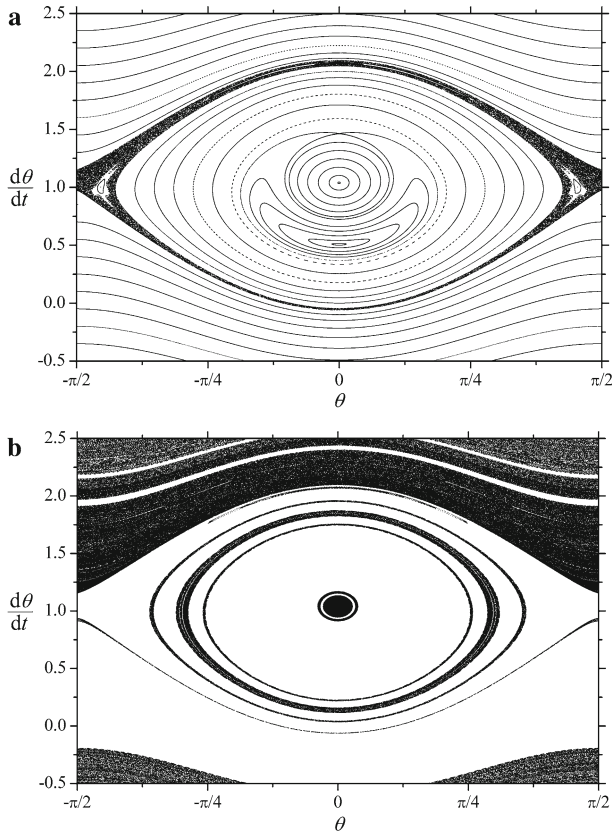
Fig. 7 The phase space section for $e = 0.002$, $\omega_0 = 1.058$ (Prometheus): **(a)** all trajectories, **(b)** only attitude stable ones

During the process of tidal capture in synchronous resonance, both satellites inevitably cross these intermittent belts of attitude instability. When such belts are present, attaining exact resonance might be more difficult in comparison with the usual situation when they are absent, because the satellite would tend to deviate from planar rotation in these zones, due to the attitude instability. So, one can put forward a hypothesis that these belts might form "barriers" for capturing the satellites in synchronous rotation. Some numerical-experimental as well as theoretical work is necessary to infer whether this hypothesis is right or not. In particular, it is necessary to compare the timescale of developing the attitude instability in a belt with that of crossing the belt due to tidal evolution.

4 Preferred orientation in chaotic rotation

In a theoretical research (Kouprianov and Shevchenko 2005) it was found that Prometheus and Pandora are likely to be in a state of chaotic rotation. An important problem is whether there exists a preferred orientation of the satellites in chaotic rotation, or their "chaotic tumbling" is isotropic? This is important for drawing conclusions about the character of rotation from observational data.
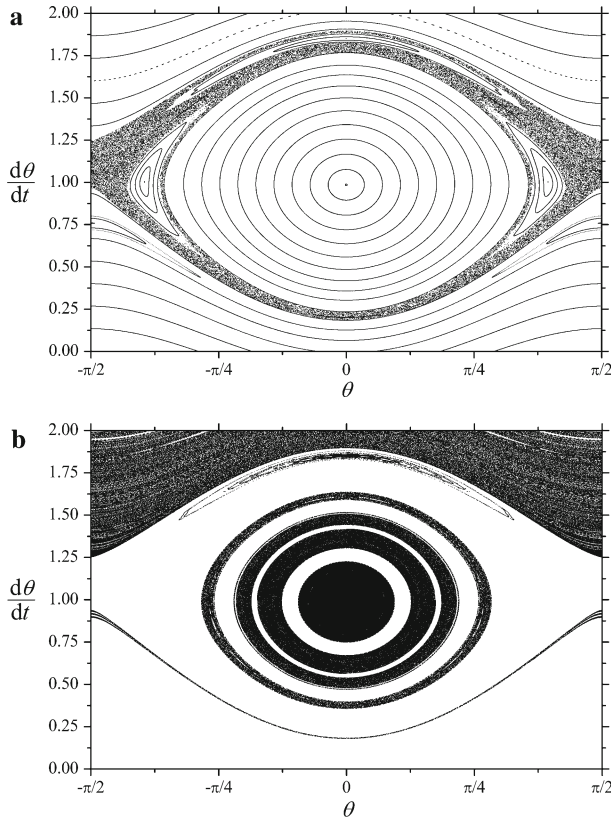
Fig. 8 The phase space section for $e = 0.004$, $\omega_0 = 0.812$ (Pandora): **(a)** all trajectories, **(b)** only attitude stable ones

For describing rotation of a satellite we use a set of Euler angles adopted in Wisdom (1987). It is different from that used above. The reason for the change is that the anisotropy of orientation with respect to the direction to the planet is described straightforwardly in the new set. The difference between the old set and the new one consists in the sequence of imaginary rotations by the angles from the initial position (identical to that in the old system; see above) to the actual orientation of the satellite. In the new set, the rotation is made first by θ about c, second, by ϕ about b, third, by $-\psi$ about a, until the axes of inertia of the satellite coincide with the actual orientation.

Therefore the angle ϕ in the new set is the angle between the largest axis of satellite's figure (the axis of the minimum moment of inertia) and the orbit plane, and the angle $(\theta - f)$ is the angle between the direction to the planet and the plane containing the largest axis of satellite's figure and orthogonal to the orbit plane.

Wisdom (1987) constructed projection of a chaotic trajectory of spatial rotational motion of Phobos to the plane $(\phi, \theta - nt)$, where n is the orbital mean motion (see Fig. 5 in (Wisdom 1987); note that $\theta - f \approx \theta - nt$ for small eccentricities). The rotation of Phobos with the model initial conditions close to the separatrices of the 1:2 spin–orbit resonance was considered. Planar rotation of Phobos is unstable with respect to tilting the axis of rotation not only near the separatrices of this resonance, but also practically in the whole 1:2 resonance zone in the
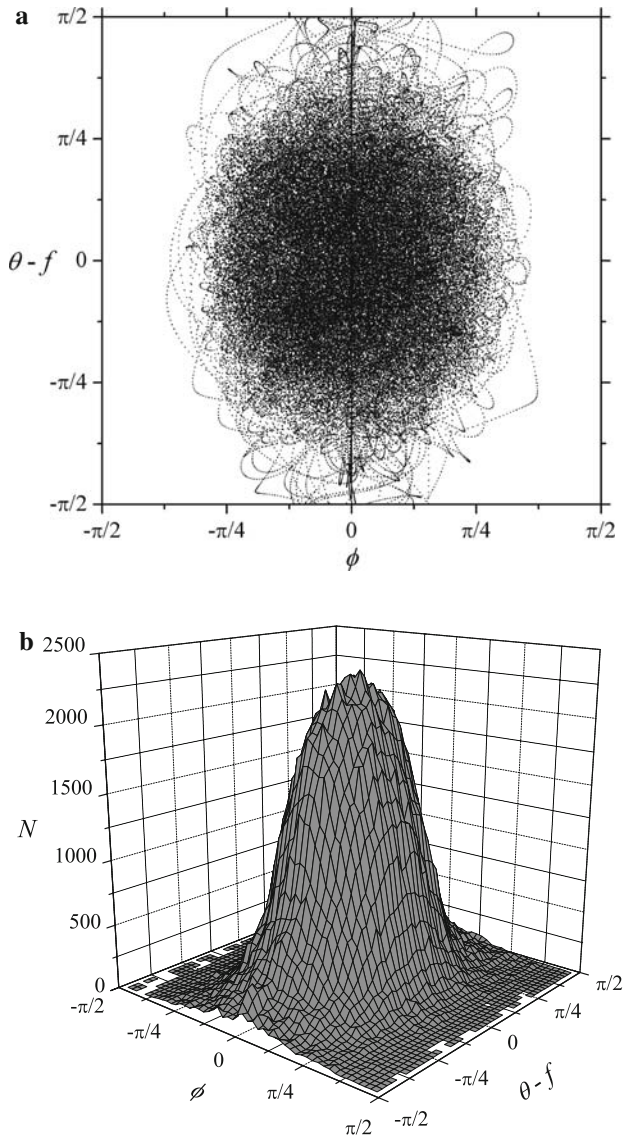
Fig. 9 Orientation of Prometheus in chaotic rotation. **(a)** Projection of the chaotic trajectory to the $(\phi, \theta - f)$ plane. The integration time is 1,000 orbital periods. **(b)** A three-dimensional density plot of the discrete projections of the trajectory to the plane $(\phi, \theta - f)$. The integration time is 10,000 orbital periods

phase space (Wisdom 1987). Figure 5 in Wisdom (1987) shows that spatial rotation of Phobos with such initial conditions is not totally chaotic: there is a preferred orientation of the largest axis of satellite's figure in the direction to the planet. Let us consider an analogous graph for the chaotic motion of Prometheus close to synchronous 1:1 resonance. In the computation we adopt the values of b/a and c/b as given in EA (1999) (see Table 1). The resulting projection of the spatial chaotic trajectory to the plane $(\phi, \theta - f)$ is shown in Fig. 9a.

Besides, in Fig. 9b, we build a three-dimensional density plot of the discrete projections of the trajectory to the plane $(\phi, \theta - f)$. The output time step is taken equal to 0.01 of the

orbital period. The square $(\phi, \theta - f) \in (-\pi/2, \pi/2) \times (-\pi/2, \pi/2)$ is divided in a grid of 40×40 pixels. The quantity N designates the number of the trajectory output points in a given pixel.

The initial data is taken inside the chaotic layer of the resonance in the phase space section of planar rotation. The graph in Fig. 9a is built for a trajectory on the time interval of 1,000 orbital periods, and that in Fig. 9b is built for the same trajectory on the time interval of 10,000 orbital periods. We present the graphs only for Prometheus; in the case of Pandora they look very similar.

The semimajor axes of the orbits of Prometheus and Pandora are equal to 139,400 km and 141,700 km, respectively (French et al. 2003); the mean radius of Saturn is equal to 57,600 km. It follows then that the relative area of Saturn's disk as seen from the satellite (with respect to the area of the celestial hemisphere) is 8.9% for Prometheus and 8.6% for Pandora. These values give the average relative time that the largest axes of figures of these satellites would be oriented in the direction to Saturn, if orientations of the satellites during the chaotic "tumbling" were isotropic. For the chaotic trajectory presented in Fig. 9 we have calculated the values of the average relative time of orientation towards Saturn; they have turned out to be equal to $\approx 30\%$ for Prometheus and $\approx 22\%$ for Pandora for the time interval of integration of 10,000 orbital periods, i.e., the "isotropic norm" is exceeded 3.3 and 2.6 times, respectively. From the plots in Fig. 9a, b and these numerical estimates it is clear that there exists preferred orientation of the largest satellites' axes in the direction to Saturn, at least for the given test trajectory.

More extensive additional test computations show that for the used time interval of integration of 10,000 orbital periods the values of the average relative time of orientation towards Saturn depend on the choice of initial data. The obtained values are in the range of 20–30%. The deviations may indicate that the observed anisotropy is a temporary effect due to specific initial conditions, and long term diffusion leads to its disappearance. This remains an open problem.

5 Conclusions

We have studied possible rotation states of two small moons of Saturn, Prometheus and Pandora. There are two different regimes of synchronous rotation in the phase space of planar rotational motion of Prometheus: α-resonance and β-resonance, i.e., it is subject to the "Amalthea effect". Pandora has α-resonance only. Our analysis of stability of planar rotation of these satellites with respect to tilting the axis of rotation has shown that α-resonance for Prometheus is unstable or close to instability, i.e., the satellite most probably cannot reside in the given regime of synchronous rotation. Rotation of Prometheus in β-resonance, as well as rotation of Pandora in its only possible α-resonance, is close to the attitude instability. Both satellites also possess period-doubling bifurcation mode of α-resonance in the phase space of rotation. Rotation of both Prometheus and Pandora in this mode is attitude unstable. With respect to multiplicity of synchronous states in the phase space, Prometheus is unique amongst the satellites with known inertial and orbital parameters. So, whether it is in chaotic rotation or not, its potential rotational dynamics are rich and complicated. To a less extent the same is true for Pandora.

Our analysis of the attitude stability of planar rotation of Prometheus and Pandora for trajectories of various sort (periodic, quasiperiodic, chaotic) on a representative set of initial data, carried out by means of computation of the Lyapunov spectra, has shown presence of alternating concentric ring-like zones of stable and unstable trajectories around the major

synchronous states for both satellites. Hypothetically, the belts of attitude instability might form "barriers" for capturing the satellites in synchronous rotation.

In a numerical experiment we have demonstrated that the satellites in chaotic rotation can mimic ordinary regular synchronous behaviour: they can have preferred orientation for long periods of time, the largest axis of satellite's figure being directed approximately towards the planet. The presence of such anisotropy of orientation of the satellites in chaotic rotation might prevent clearing up the character of rotation in observations. Whether this anisotropy is a temporary effect due to specific initial conditions, with long term diffusion leading to its disappearance, remains an open problem.

References

Beletsky, V.V.: The Motion of an Artificial Satellite about its Mass Center. Nauka Publishers, Moscow (1965)

Black, G.J., Nicholson, P.D., Thomas, P.C.: Hyperion: rotational dynamics. Icarus **117**, 149–161 (1995)

Cooper, N.J., Murray, C.D.: Dynamical influences on the orbits of Prometheus and Pandora. Astron. J. **127**, 1204–1217 (2004)

Devyatkin, A.V., Gorshanov, D.L., Gritsuk, A.N., Melnikov, A.V., Sidorov, M.Yu., Shevchenko, I.I.: Observations and theoretical analysis of light curves of natural planetary satellites. Sol. Sys. Res. **36**, 248–259 [Astron. Vestnik **36**, 269–281] (2002)

Éphémérides Astronomiques (Annuaire du Bureau des Longitudes). Masson, Paris (1999)

Farmer, A.J., Goldreich, P.: Understanding the behavior of Prometheus and Pandora. Icarus **180**, 403–411 (2006)

French, R.G., McGhee, C.A., Dones, L. et al.: Saturn's wayward shepherds: the peregrinations of Prometheus and Pandora. Icarus **162**, 143–170 (2003)

Goldreich, P., Rappaport, N.: Chaotic motions of Prometheus and Pandora. Icarus **162**, 391–399 (2003a)

Goldreich, P., Rappaport, N.: Origin of chaos in the Prometheus–Pandora system. Icarus **166**, 320–327 (2003b)

Goździewski, K., Maciejewski, A.J.: On the gravitational fields of Pandora and Prometheus. Earth Moon Planets **69**, 25–50 (1995)

Hairer, E., Nørsett, S.P., Wanner, G.: Solving Ordinary Differential Equations I. Nonstiff Problems. Springer-Verlag, Berlin (1987)

Klavetter, J.J.: Rotation of Hyperion. I—Observations. Astron. J. **97**, 570–579 (1989a)

Klavetter, J.J.: Rotation of Hyperion. II—Dynamics. Astron. J. **98**, 1855–1874 (1989b)

Kouprianov, V.V., Shevchenko, I.I.: On the chaotic rotation of planetary satellites: the Lyapunov exponents and the energy. Astron. Astrophys. **410**, 749–757 (2003)

Kouprianov, V.V., Shevchenko, I.I.: Rotational dynamics of planetary satellites: a survey of regular and chaotic behavior. Icarus **176**, 224–234 (2005)

Kouprianov, V.V., Shevchenko, I.I.: The shapes and rotational dynamics of minor planetary satellites. Sol. Sys. Res. **40**, 393–399 [Astron. Vestnik **40**, 428–435] (2006)

Markeev, A.P.: Theoretical Mechanics. Nauka Publishers, Moscow (1990)

Melnikov, A.V.: Bifurcation regime of synchronous resonance in the transitional-rotational motion of nonspherical natural satellites of planets. Cosmic Res. **39**, 68–77 [Kosmich. Issled. **39**, 74–84] (2001)

Melnikov, A.V., Shevchenko, I.I.: The stability of the rotational motion of nonspherical natural satellites, with respect to tilting the axis of rotation. Sol. Sys. Res. **32**, 480–490 [Astron. Vestnik **32**, 548–559] (1998)

Melnikov, A.V., Shevchenko, I.I.: On the stability of the rotational motion of nonspherical natural satellites in synchronous resonance. Sol. Sys. Res. **34**, 434–442 [Astron. Vestnik **34**, 478–486] (2000)

Melnikov, A.V., Shevchenko, I.I.: Unusual rotation modes of minor planetary satellites. Sol. Sys. Res. **41**, 483–491 [Astron. Vestnik **41**, 521–530] (2007)

Porco, C.C., Weiss, J.W., Thomas, P.C., Richardson, D.C., Jacobson, R.A., Spitale, J.: Physical characteristics and possible accretionary origins for Saturn's small satellites. 37th Annual Lunar and Planetary Science Conference. Abstract No. 2289 (2006)

Seidelmann, P.K., Abalakin, V.K., Bursa, M., Davies, M.E., de Bergh, C., Lieske, J.H., Oberst, J., Simon, J.L., Standish, E.M., Stooke, P., Thomas, P.C.: Report of the IAU/IAG working group on cartographic coordinates and rotational elements of the planets and satellites: 2000. Celest. Mech. Dyn. Astron. **82**, 83–110 (2002)

Seidelmann, P.K., Archinal, B.A., A'Hearn, M.F., Cruikshank, D.P., Hilton, J.L., Keller, H.U., Oberst, J., Simon, J.L., Stooke, P., Tholen, D.J., Thomas, P.C.: Report of the IAU/IAG working group on cartographic coordinates and rotational elements: 2003. Celest. Mech. Dyn. Astron. **91**, 203–215 (2005)

Seidelmann, P.K., Archinal, B.A., A'Hearn, M.F., Conrad, A., Consolmagno, G.J., Hestroffer, D., Hilton, J.L., Krasinsky, G.A., Neumann, G., Oberst, J., Stooke, P., Tedesco, E.F., Tholen, D.J., Thomas, P.C., Williams, I.P., Cruikshank, D.P., Hilton, J.L., Keller, H.U., Oberst, J., Simon, J.L., Stooke, P., Tholen, D.J., Thomas, P.C.: Report of the IAU/IAG working group on cartographic coordinates and rotational elements: 2006. Celest. Mech. Dyn. Astron. **98**, 155–180 (2007)

Shevchenko, I.I.: The separatrix algorithmic map: application to the spin-orbit motion. Celest. Mech. Dyn. Astron. **73**, 259–268 (1999)

Shevchenko, I.I., Kouprianov, V.V.: On the chaotic rotation of planetary satellites: the Lyapunov spectra and the maximum Lyapunov exponents. Astron. Astrophys. **394**, 663–674 (2002)

Stooke, P.J.: The shapes and surface features of Prometheus and Pandora. Earth Moon Planets **62**, 199–221 (1993)

Thomas, P.C.: The shapes of small satellites. Icarus **77**, 248–274 (1989)

Thomas, P.C., Black, G.J., Nicholson, P.D.: Hyperion: rotational dynamics. Icarus **117**, 128–148 (1995)

von Bremen, H.F., Udwadia, F.E., Proskurowski, W.: An efficient QR based method for the computation of Lyapunov exponents. Physica D **101**, 1–16 (1997)

Wisdom, J.: Rotational dynamics of irregularly shaped natural satellites. Asron. J. **94**, 1350–1360 (1987)

Wisdom, J., Peale, S.J., Mignard, F.: The chaotic rotation of Hyperion. Icarus **58**, 137–152 (1984)